Project title: Intertemporal choice across short and long time horizons: an fMRI study

Evgeniya Lukinova[1,2], **Shengjie Xu**[1], **and Jeffrey C Erlich**[1,2,3]

[1]**NYU Shanghai, 1555 Century Avenue, Shanghai, 200122, China**
[2]**NYU-ECNU Institute of Brain and Cognitive Science at NYU Shanghai, 3663 Zhongshan Road North, Shanghai, 200062, China**
[3]**Shanghai Key Laboratory of Brain Functional Genomics (Ministry of Education), East China Normal University**

This document describes an fMRI study pre-registered at OSF (http://OSF.io).
This study was registered prior to creation of data.

Keywords: intertemporal choice, time horizons, fMRI

CONTENTS

1 INTRODUCTION

Individual's intertemporal preferences in the lab are predictive of important real life outcomes (Mischel et al., 1989; Golsteyn et al., 2014; Watts et al., 2018), which has motivated economists, psychologists and neuroscientists to investigate the behavioral and biological bases of discounting in humans and non-human animal models. However, there are two key differences in methods across species which create a gap between human and non-human studies: (i) verbal vs. nonverbal stimuli and (ii) long (days, months) vs. short (minutes, seconds) delays. Our recent study (Lukinova et al., 2019) established high reliability across the verbal/non-verbal gap and moderate reliability across the long/short delay gap. Moreover, we found a 5 order of magnitude increase in discount rates in the short vs. long tasks. From a neoclassical economics perspective this increase may appear unbelievable: e.g., the same individual who decides to wait for 15 days for twice award declines to wait 30 seconds for twice the award.

This fMRI study is designed to further explore the long/short gap. There are numerous long delay incentive-compatible fMRI studies (e.g., McClure et al., 2004, 2007; Kable and Glimcher, 2007; Ballard and Knutson, 2009; Kable and Glimcher, 2010; van den Bos et al., 2014; Massar et al., 2015; Chen et al., 2019) as well as short delay experiential ones (Gregorios-Pippas et al., 2009; Prevost et al., 2010; Wittmann et al., 2010; Onoda et al., 2011; Jimura et al., 2013; Tanaka et al., 2014), some of which examined neural correlates of the waiting epoch in the short delay task. Nevertheless, to our knowledge there are no fMRI studies that investigate time preferences within subject across time scales. Our within-subject design gives us an advantage: contrasting short delay task block and long delay task block within runs of individual subjects should reveal differences between intertemporal choices that involve waiting vs. postponing (Paglieri, 2013).

2 AIMS & HYPOTHESES

The main goal of this study is to reveal the overlapping and distinct neural circuitry underlying intertemporal choices that involve waiting for reward vs. postponing reward. Here, we use 'waiting' to refer to decisions where the delays are short and experienced and 'postponing' to refer to rewards which are put off until a future time, but other activities fill the delay duration. An example of a decision involving waiting in day to day life is choosing whether or not to pay to skip an advertisement before watching the video you want to watch. An example of a decision involving postponing might be choosing to pay for next day delivery from an online shop or waiting a week for free delivery.

At least three neural systems play a role in delay discounting: valuation, prospection and executive control. To date, most attention in fMRI studies on delay discounting has been focused on the valuation network (Lempert et al., 2018), in particular, Kable and Glimcher (2007) show that "neural activity in several brain regions—particularly the ventral striatum, medial prefrontal cortex and posterior cingulate cortex—tracks the revealed subjective value of delayed monetary rewards". We expect to replicate this finding, but also to see differential interactions between valuation, prospection and executive control in the short vs. long tasks.

Our main hypotheses are as follows:

1. Overlapping brain activation will be found both in short and long temporal contexts, especially in the valuation network (ventromedial prefrontal cortex, ventral striatum and posterior cingulate cortex). Out of six papers cited in relation to incentivized intertemporal choice task with waiting and 12 papers with postponing all (18) report activation in valuation network (14 report activation at least in striatum).

2. Less overlap between waiting and postponing in valuation, executive control and prospection networks will be observed for those subjects whose discount factor in short delay and long delay tasks are furthest from the line of best fit of $\log(k_S)$ vs. $\log(k_L)$ across subjects. E.g. A subject who is patient in the short task but impulsive in the long task will have less overlap than a subject who is patient in both tasks (or impulsive in both tasks).

3. We strongly expect to replicate the commonly found positive parametric modulation of the valuation network by reward magnitude (for delayed option), by the inverse delay of the delayed reward and by subjective value at the time of choice (as in Kable and Glimcher, 2007).

4. On the individual level we strongly expect to replicate the finding from Ballard and Knutson (2009) that "more impulsive subjects show less neural sensitivity to the larger magnitudes of future rewards but greater (negative) neural sensitivity to the longer delays of future rewards."

In addition to our main hypotheses, we have several weaker predictions based on less well replicated results in the literature:

1. We anticipate negative parametric modulation of dorsolateral prefrontal cortex (executive control network) by delay during the choice (at least for long delays, as in Ballard and Knutson, 2009).

2. We anticipate positive parametric modulation of anterior prefrontal cortex (prospection network) by the delay during the waiting period (reflecting the delay-period dynamics in Jimura et al., 2013).

3. We anticipate that engaging in waiting compared to postponing will reveal widespread activation in regions involved in executive control network (dorsolateral prefrontal cortex and dorsal anterior cingulate cortex), stronger in Short than in Long (since it will engage working memory more, as in van den Bos et al., 2014).

4. We ancticipate that engaging in waiting compared to postponing will also reveal activations in prospection network (medial temporal lobe, precuneus, and dorsomedial prefrontal cortex) and the signal will be stronger in Long than in Short (since prospection reduces discounting, as in Peters and Büchel, 2010; Palombo et al., 2015).

3 DATA COLLECTION PROCEDURES

Data collection will be done according to the approved IRB protocol (024-2017) at NYU Shanghai. Thus, information below is copied from the approved protocol.

Subjects will not be included or excluded on the basis of the following characteristics: gender, race, ethnic origin, religion, social or economic factors.

All of the following criteria must be met for inclusion in computer and fMRI sessions of this study: (1) the participant is able to understand instructions and is willing to comply with the requirements in this study; (2) the participant has signed the Consent Form for this study; (3) the participant is 18 or older; (4) the participant passes the 3T MRI Security Screening; (5) the participant is right-handed (screening questionnaire, consent and IRB approval attached as separate documents).

We will exclude subjects that indicate any risk factor (do not pass the screening) in the 3T MRI Security Screening questionnaire administered prior to participation in the fMRI session.

The following participants will be excluded from computer and fMRI sessions of this study: (1) any participant for whom informed consent cannot be obtained; (2) participants with known history of neurological diseases, traumatic brain injury, psychiatric illness, drug/alcohol abuse, or eye disease; (3) pregnant women; (4) participants who are left-handed; (5) any participants younger than 18.

Subjects will be recruited from the student population of NYU Shanghai and East China Normal University. Subjects will be informed of the opportunity to participate through recruitment flyers (attached as a separate document). The recruitment flyers will be posted on the university website and campus bulletin boards. Recruitment will be also done through posting flyers in WeChat (ECNU subjects pool tools' recruitment). Subjects that are willing to participate in the study can scan QR code, read the brief intro and fill in the registration form. Chinese subjects will fill in all forms and see stimuli in Chinese, subjects of other nationalities will fill in all forms and see stimuli in English.

Prior to the start of the study, participants will fill out and sign the informed consent form. Then, in the first session they will fill out the personality questionnaire (Barratt impulsiveness scale (BIS) attached as a separate document) and participate in a behavioral testing session in order to estimate their discount factor. Subjects will be making decisions on a computer. They will earn coins and will be compensated based on the participation rate and the coins they earned at the session.

Some subjects may not be invited to the fMRI session due to: 1) fMRI safety considerations; 2) scientific justification: researcher's goal to cover diverse time preferences given limited resources for fMRI session. In other words, we will use the behavioral testing session to estimate subjects discount factors and we will choose a subset of subjects which span a range of discount factors (Lukinova et al., 2019) so that we can have an appropriate amount of variability for fMRI data analyses. For the scanning

session, participants will have to pass the screening questionnaire and then will make decisions in the scanner with the experimental stimuli similar to computer session. For the scanning sessions, participants will be instructed to remove all metal objects before entering the magnet room. After entering the MRI magnet room, they will be given earplugs and noise-reducing headphones to wear to shield them from the noise of acquiring images on the MRI scanner. Foam pads will be placed around their heads to limit head movement during the scan. The table will then be slid into the scanner so that the head and upper body are inside the magnet tube. Following each scanning run, the researcher operating the MRI scanner will ask the participants how they are doing and if they want to continue. If they like, participants can take a brief rest in the scanner and then continue. During the scanning, participants will be asked to hold still, and listen to sounds, watch visual stimuli and respond by pressing a button. Participants can decide to stop at any time and the experimenter will take them out. After subjects are taken out they are compensated for participation and in addition dependent on the number of the coins they got during the session.

The total time for participation in the computer session will take from 1 hour to 1.5 hours. The total time for participation in the scanning session will take approximately 1.5 hours, including about 15 minutes for filling out forms. Subjects will be compensated for 20 RMB for any level of participation for computer session and for 100 RMB for scanning session. In addition they can receive from 0 RMB up to 50 RMB through the reward system tied to the experimental task. There is no cost to any participant associated with participation in this study. If a subject withdraws prior to the end of the study we will pay him/her based on the compensation rate and the experimental task reward system at the time he/she quits.

The behavioral criteria we will use to determine whether to invite subjects to the fMRI session or not are the following: (i) subjects make at least 10% choices of 'immediate' and 'delayed' category in both Short and Long tasks, (ii) subjects are sensitive to reward and delay (details in section 'Measured Behavioral Variables').

3.1 Sample Size & Stopping Rule

The target sample size (for the fMRI session) is 40 participants. Standard fMRI study includes around 30 participants, e.g., 27 (as in Hare et al., 2014) and 32 (as in Tanaka et al., 2014) after discarding subjects whose data contains too many artifacts. No power analysis is used to set the sample size. The target sample size was set based on funding constraints. We estimated that our effect size would be comparable to previous within-subjects studies of intertemporal choice (Peters and Büchel, 2010). In the case of logistical issues (equipment or research staffing) we may stop the study after collecting as few as 30 subjects. We will not analyze the data (beyond preprocessing) until all subjects data have been collected.

4 MEASURED BEHAVIORAL VARIABLES

In our delay task, two options will be presented on the screen on each trial: a delayed option and an immediate option. Subjects will make a choice (*choice* is a binary variable, where 1 is for delayed option and 0 for immediate option) given reward magnitude of both options (*reward* for delayed option (The immediate option reward is always 4 coins) and delay (*delay* in the units of the task, i.e. seconds or days) of the delayed option.

We will first measure these variables for those who participate in the computer session and decide whether to invite them or not to the subsequent fMRI session. We will obtain $choice, reward, delay$ variables per trial of behavioral task and will first check whether for each task (within computer session) $0.1 \leq mean(choice) \leq 0.9$ and both p-values (for *reward* and $delay$ coefficients) in the regression ($choice \sim reward + delay$) are significant. In other words, subjects are excluded if they always choose the delayed (or immediate) option or if they are insensitive to either delay or reward.

We will get the following variables for subjects who participate in both computer and the subsequent fMRI sessions:

- variables collected per trial $choice, reward, delay$;
- variables estimated via model fits per session, per subject: discount factors $\log(k_S)$, $\log(k_L)$ and decision noise τ (following procedures from Lukinova et al., 2019). "Subjects' impulsivity was estimated by fitting their choices with a Bayesian hierarchical model (BHM) of hyperbolic discounting with decision noise." The model has four population level parameters (log discount factor, $\log(k)$, and decision noise, τ, for each of the two tasks, also known as fixed effects) and three parameters per subject: $\log(k_S)$, $\log(k_L)$, and τ.

After estimation of discount factors, subjective value (SV) can be calculated for the delayed option per trial, per task, per subject, where individual subjective value of the delayed reward is assumed to be hyperbolic $SV = \frac{V}{1+k_{i,task}T}$, where V is the current value of delayed asset (*reward*), T is the delay time ($delay$), $k_{i,task}$ represents the discount factor for the i^{th} subject in either the short or long $task$.

Moreover, we will record subject's decision response time (RT), side (left or right) of the decision, exact intertrial interval (ITI) onset and duration, onset time of each trial, onset and duration of each event in the trial, time and date of the session.

In Lukinova et al. (2019) we did not find any significant relationships between discount factor and gender, undergraduate major or BIS. Nevertheless, subjects will also answer questions about their age, gender, major and impulsivity (BIS). Responses to these questions will be used to test that our previous null results are replicated.

If participants fail to make a choice given the time limit the choice will randomly made by the computer. Participants are instructed that their final earnings might be dependent on that choice. Those trials will not be included in analyses.

We will directly estimate the natural log of k, $\log(k)$, and not k as a model parameter because we found that k is approximately log-normally distributed over subjects previously (Lukinova et al., 2019). No re-coding of the data is planned for the confirmatory analyses.

4.1 Analysis Data Exclusion

Even after not inviting some of the subjects from computer session to the fMRI session we still may find some subjects are either (a) not making enough choices of delayed or immediate options or (b) failing to make choices in the given time limit. For the former, the same criteria (as after computer session) will be used for fMRI subjects data exclusion: we will exclude subject data if for any of the tasks $0.1 \leq mean(choice) \leq 0.9$. For the latter, we will include those subjects, whose data has less than 10% missing button presses. Missing button presses trials will be excluded from analyses.

Before running preprocessing, several quality checks will be implemented to ensure that results are not influenced by artifacts. We will perform quality control of MRI data in two ways: i) a quantitative check with 'mriqc' package (version 0.15.0) at group level to have both individual metrics and group-level analysis to find outliers across all subjects (Esteban et al., 2017) and ii) a visual qualitative check. If a BOLD run does not pass this check (checklist is attached), this BOLD run will be removed from further analysis. If more than two runs are excluded for a single subject, we will exclude that subject. If a structural T1-weighted scan does not pass this check, we will also exclude that subject.

(1) Quantitative checks: 'mriqc' generates group reports for structural and BOLD data. We will exclude subject's data (both structural and BOLD) if the data is detected as an outlier in any structural or functional metric (detailed list is available in the metrics document attached and in the official 'mriqc' documentation). Special emphasis will be put on head motion, including a) increasing trends of motion, b) fd_num (the number of timepoints above framewise displacement threshold of 0.2mm) being an outlier in the group report, or c) mean head motion is over 0.2mm.

(2) Qualitative checks: All qualitative checks will be done according to Center for Brain Science (Harvard University) quality control manual (document attached and available online). We will check the data visually for wrapping, signal loss, ringing, striping, blurring, ghosting, etc. If there is a noticeable dropout in the orbitofrontal cortex by visual scrutiny (the area where regions of interest are located) participant's data will be excluded. These steps depend on the trained eye and the experience of each reviewer, thus, at least two researchers from the project will train their eyes to get familiar with each type of artifacts and follow the guidelines of the control manual.

5 EXPERIMENTAL DESIGN

At first, all subjects participate in the computer session and they may or may not be invited to the fMRI session on a separate day. The tasks and the stimuli appearance used across the sessions are the same. This is a within-subject study, so all participants do exactly the same tasks (in a different order, described later). We use a mixed design type, i.e. a block design with events within the blocks. Two tasks (Short Delay Task (S) and Long Delay Task (L)) are used in this study. In the computer session, subjects will do 100 trials of each task (200 trials total) divided into 2 runs (2 blocks(tasks) per run) of 50 trials of S and 50 trials of L each in an interleaved fashion: S-L-S-L or L-S-L-S for half of the subjects (similar to

Lukinova et al., 2019). In the fMRI session, subjects will also do 100 trials of each task (200 trials total), divided into 4 runs (2 blocks(tasks) per run) of 25 trials of S and 25 trials of L each in an interleaved fashion: S-L-L-S-S-L-L-S or L-S-S-L-L-S-S-L. Therefore, we plan to acquire a total of 200 trials per subject per session. The total length of experiment is defined in the IRB protocol as between 1-1.5 hours, including filling in the forms. The total length of S is directly dependent on subject's choices, i.e. whether he decided to (actively) wait or not. The choice sets (rewards and delays) are optimized to be able to fit the diverse time preferences of subjects (the simulation is described in the section below). The tasks are coded in PsychoPy toolbox (3.1.5, (Peirce, 2007)) and run on a Windows 7 laptop. The payment for experiment is incentive-compatible. Following Lukinova et al. (2019) we compensate subjects according to their real choices (in S all trials are counted for payment, 1 coin = 0.02 RMB; in L one trial is chosen randomly for payment, 1 coin = 2 RMB).

5.1 Design Optimization

The task choice set was optimized to be able to fit diverse subjects' discount factors ($\log(k)$). We created 50 agents with known $\log(k)$, by generating uniformly distributed numbers in the range of [-9 1] (resembling the range of real discount factors from the main experiment in Lukinova et al. (2019)) and by generating uniformly distributed numbers in the range of [0.5 1] for decision noise τ. Then, we created 5000 random choice sets of 50 trials each, with reward range in [5:1:15] (from 5 to 15 with increment of 1) and for the delay 10% of values were in the range of ([30:1:60] seconds), 20% in the range of [15 30] and the rest in the range of [1 15]. This way, expected delay average is (30+60)/2*10%+(15+30)/2*20%+(1+15)/2*70% = 14.6, close to 13.3 of our original set from delay study (Lukinova et al., 2019). Given each of the choice sets 50 agents made simulated choices (simulated data, 5000*50*50 = 12,500,000 observations). Then, given simulated data we fit the hyperbolic model with softmax individually per each agent (following the procedure for individual fits in matlab in Lukinova et al. (2019)) and check how well we can recover ($\log(k)$). The best set gives us $R^2 = .75$. We did not accurately recover the $\log(k)$ when the true value was < -6, but these subjects should be excluded before fMRI session since the average $mean(choice) > .95$ for them given our choice set. Among five best sets by R^2 (Figure 1), set #4 gives us the smallest mean delay of 13.42 and $R^2 = .736$, therefore, we choose this broad choice set (attached) for the short delay task in the computer session and fMRI session.

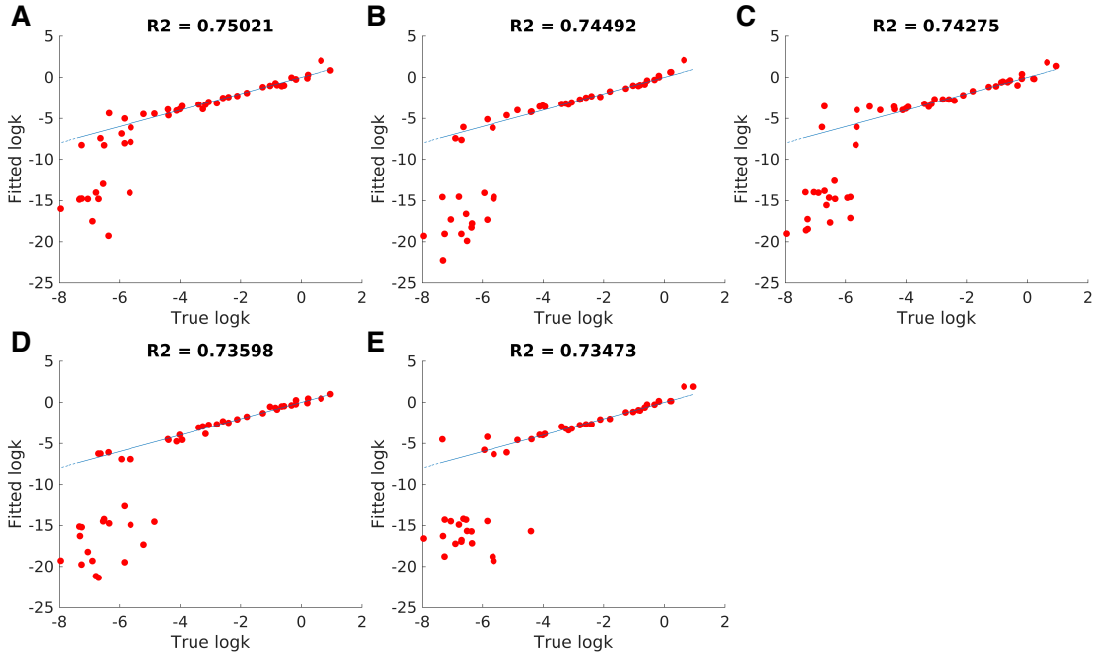

Figure 1. Parameter Recovery. Each plot shows how well we can recover $\log(k)$ given 5 best choice sets (respectively, A, B, C, D and E) ordered by R^2 (how well the dots fit the unity ($x = y$) line). The x-axis portrays the true $\log(k)$ of the k-agent, while y-axis - recovered $\log(k)$. Each dot is a k-agent. The recovered $\log(k)$ is way off for the smaller values, i.e. $\log(k) < -6$.

For the long delay task in both computer and fMRI sessions we repeat the procedure above, but use a wider range for delay values [5:1:150] (days) and select the best choice set by R^2 ($R^2 = .926$).

5.2 Task Specification

The timeline and expected trial duration of the L and S tasks are shown in Figure 2 and Figure 3, respectively.

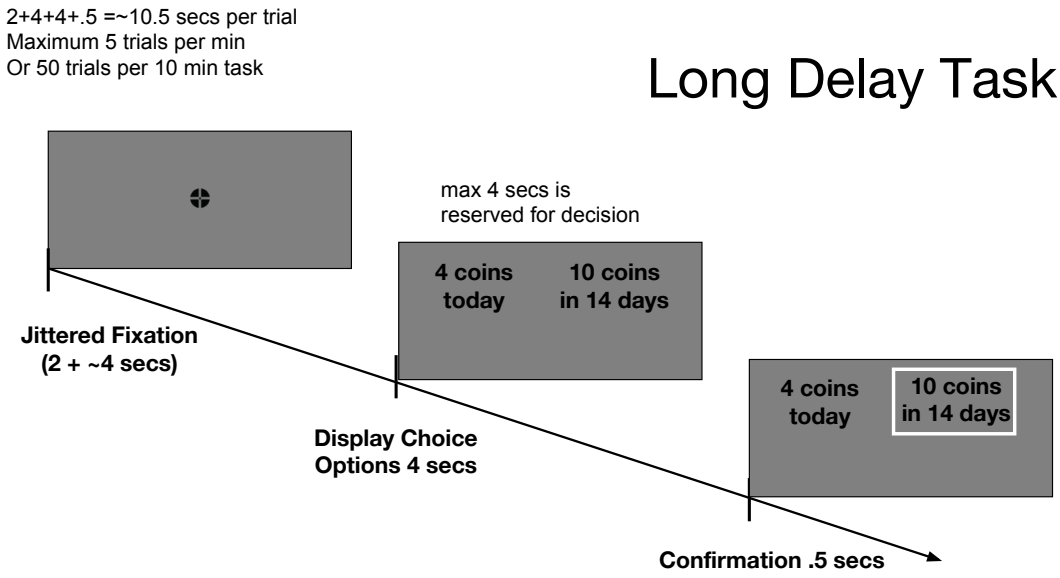

Figure 2. A timeline of the long delay task.

Within each task the following events are considered for analysis:
- Fixation
- Decision(decision(immediate)+decision(delayed))
- Confirmation
- Waiting (only in Short Delay task)
- Coins (only in Short Delay task)

The instructions for the computer and the fMRI sessions are attached as separate documents. The responses for fMRI session are collected using a button box placed in participant's right hand, where left choice was attached to button #1 (index finger) and right choice was attached to button #2 (middle finger) (computer session - keys 'left arrow' and 'right arrow' on the keyboard, respectively).

All subjects will experience stimuli from the optimal sets (both broad short and long) of 50 trials each in four pseudorandom orders (two orders per short and two orders per long task, distributed randomly and roughly equally across subjects) : A, B, C, D (exact orders attached). This design means that half of the subjects start with Short (Long) and half of those experience starting order A (C) to rule out possible anchoring effects (that can set a reference point in the early part of the experiment and guide choices throughout the rest as in Tversky and Kahneman, 1974; Wilson et al., 1996; Furnham and Boo, 2011). The Table 1 below further explains how orders will be distributed among the tasks in a session. The pseudorandom order is determined in such a way that two halves of the randomized set are moderately equal (difference between the means of reward and difference between the means of delay < 1 unit), since in fMRI session the run consists of 25 trials.

	first Short	first Long
first A	SA-LB-SC-LD	LA-SB-LC-SD
first C	SC-LD-SA-LB	LC-SD-LA-SB

Table 1. Pseudorandom Order of Trials in a Run

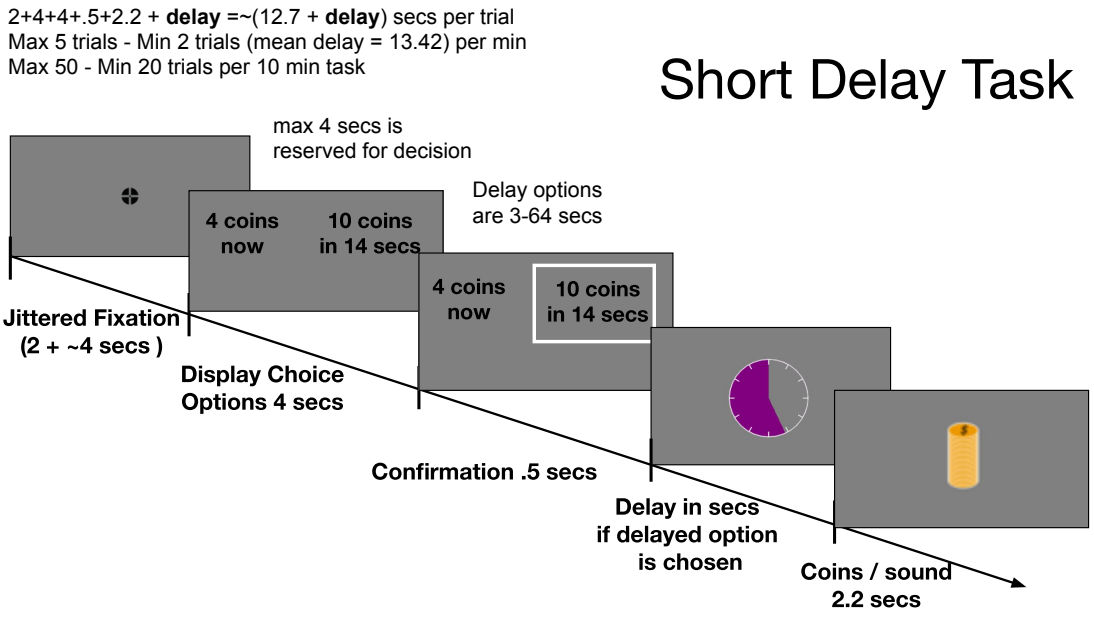

Figure 3. A timeline of the short delay task.

6 DATA ACQUISITION

At least two research assistants will interact with subjects for computer and fMRI sessions. First, the localizer and the structural scan sequences are run, in this order. Then, fMRI scanning is divided into four functional runs. The fMRI technician is asked to set the scan time to 20 mins, but the actual duration of the scan differs depending on the subject's choice to wait or not. The technician is asked to stop scanning when one run of the behavioral task is over. After two runs, subject can relax, if necessary.

Functional MR images (whole brain) will be obtained for each subject by using Siemens Prisma 3T system in the Neuroimaging Center of East China Normal University (ECNU). Images will be acquired by using echo-planar T2 images (EPI, gradient echo (GRE), using Simultaneous Multi-Slice (SMS) package: GRAPPA 2, MB 2, No PF) with BOLD (blood oxygenation-level-dependent) contrast, and angled 30° with respect to the AC-PC line to minimize susceptibility artifacts in the orbitofrontal cortex (Deichmann et al., 2003). MR imaging settings are as follows: repetition time (TR) = 1,740 ms; echo time (TE) = 27.0 ms; slice thickness = 3 mm yielding a 64 x 64 x 42 matrix (3 mm x 3 mm x 3 mm); flip angle = 90°; FOV read = 192 mm; FOV phase = 100 %, interleaved series order (the exact sequence parameters are in the attached file). The EPI sequence was optimized to reduce the dropoff in OFC area. High-resolution structural T1-weighted scans (0.9 mm x 0.9 mm x 0.9 mm) will be acquired by using an MPRage sequence. Visual stimuli will be presented by means of a mirror mounted on the MRI head coil, and responses will be acquired via an MRI-safe 5-button response box (Sinorad).

7 PREPROCESSING

All MRI data collected will be in DICOM format that will be converted into 4d NIfTI format (BIDS) by using 'dcm2nii' (through 'MRIcroGL'). The data then will undergo a QC monitoring (described in detail in section 4.1) by using the quantitative metric ('mriqc') and with a trained eye. Next, we will use '3dDespike' (default options) from AFNI (Analysis of Functional NeuroImages, version 19.1.08 'Caligula' Cox (1996)) to remove 'spikes' from the data that has fd_num>0 (from QC), i.e. data that has some spikes due to motion. This software "writes a new dataset with the spike values replaced by something more pleasing to the eye" and stores the data in the AFNI data format (BRIK+HEAD). To convert back to the BIDS format for preprocessing we will use '3dAFNItoNIFTI' (AFNI).

Since we are going to do QC of subjects structural images we may observe an anomaly. This is the exact notice we have on incidental findings in the consent form of the approved IRB protocol:

INCIDENTAL FINDINGS

Note that MRI is commonly used in medicine for the purpose of diagnosing abnormalities of the brain. The procedures that are to be used in this study are different from clinical MRI scanning. As researchers, we do not intend to make any medical diagnosis with the MRI as used in this research project, and we are not trained in medical diagnosis. However, if in the course of this research study we observe an anomaly in one or more of the MRI images, we feel ethically obligated to inform you of the observation. We believe it is important to inform you of such observations, because we cannot rule out the possibility that an anomaly may require medical attention. In this event, all information collected as part of this study will be made available to you for further examination by a medical professional. You will be fully responsible for the costs associated with a radiological examination and any further examinations or treatments that may be required for medical purposes. If you prefer not to be informed of an image anomaly, you must choose not to participate in the study.

We will use standard pipeline for preprocessing, as specified in fmriprep (version 1.4.1), 'minimal preprocessing' including motion correction, field unwarping, normalization, bias field correction, and brain extraction (Esteban et al., 2019). Table 2 includes all preprocessing steps available in the package and used by default. To the default preprocessing options we will add Susceptibility Distortion Correction (SDC) - a filedmap-free method to correct distortion.

Anatomical Preprocessing	Functional Preprocessing
Fuse & Conform	Generate reference & brain mask
Intensity nonuniformity (INU) correction	Estimation of head-motion
Skull-stripping	Slice-timing correction, susceptibility distortion estimation
Spatial normalization, brain tissue segmentation, surface reconstruction	$\longrightarrow$ Alignment to T1 reference

Table 2. fmriprep: A standard pipeline for preprocessing.

8 STATISTICAL MODELING

8.1 GLM

We will use FSL (FMRIB Software Library v6.0, www.fmrib.ox.c.uk/fsl (Jenkinson et al., 2012)) FEAT, FMRI Expert Analysis Tool (Woolrich et al., 2001), for first level analyses, i.e. per subject, per run. In order to perform FEAT and skip registration (which is already done in fMRIprep) we will follow instructions in the video from Jeanette Mumford, i.e. prevent image from moving (by using identity matrix) and interpolating again (by overwriting the standard). fMRI data will be pre-whitened with FSL FILM, FMRIB's Improved Linear Model, the time-series modelling tool used within FEAT, where autocorrelation function is estimated at each voxel to account for temporal autocorrelation (Woolrich et al., 2001). Six motion regressors and FD (calculated via 'fsl_motion_outliers' tool) for each TR will be included as regressors of no interest. All main regressors will be described later for each model separately, each convolved with a canonical hemodynamic response function (HRF, Double-Gamma) and modeled with boxcars having the durations of the corresponding event (unless specified otherwise). Since we have several runs per subject, on the second level we will use a fixed effects model (as opposed to mixed effects, in fixed effects reported activation is with respect to the group of runs present, and not representative of the wider population; it assumes a common run-to-run variance). We will use FEAT for second level analysis, by forcing the random effects variance to zero in FLAME (FMRIB's Local Analysis of Mixed Effects) to average contrast estimates over runs within subject. Then, the resulting individual subject mean response (fixed effect model result for each contrast) will enter the group level analysis (mixed effects analysis includes random effects for each subject and, thus, takes into account inter-subject variability). Group results on the third level will be conducted using FSL FLAME 1 with a cluster-forming threshold of $z > 2.3$ and $p < 0.05$ (corrected for multiple comparisons). In order to address our hypotheses we construct three general linear models for the planned analyses with the following steps described in detail above:

1. the first level analysis: single run, single subject (FEAT)
2. the second level analysis: multiple runs, single subject (FEAT)

3. the third level analysis: group level analysis (FEAT FLAME 1)

In the first model (GLM1), we will do a localization analysis of temporal context, i.e. locate areas that correspond to waiting (and short task in general) versus postponing. This model will address the main hypothesis 1 (overlapping brain activations for both tasks in valuation network), hypothesis 2 (less overlap between short and long tasks for those subjects further away from the fitted line of $\log(k_S)$ vs. $\log(k_L)$) and weaker hypotheses 3 and 4 (activations in executive control and prospective networks, respectively). We will model decision (from the onset of the event) and confirmation (from onset of confirmation until the onset of the new trial) events in a corresponding trial, resulting in two events in each task. Therefore, the design matrix (Table 3) will contain four regressors of interest. Eight linear contrasts of regression coefficients will be computed. We will use contrasts 1-4 on the first level as MVPA inputs. The same contrasts on the group level will generate Z statistic images for each of the regressors of interest. Contrasts 5, 7 (6, 8) will show where activations are stronger for Short (Long). On the group level (single group, one-sample t-test) we will answer the question: does the group activate on average? - and will specifically address the main hypothesis 1. Considering two groups (closest to the fitted line of $\log(k_S)$ vs. $\log(k_L)$ and furthest, two-sample t-test) and answering the question: is there a significant group difference? - will relate to the main hypothesis 2.

Regressors ->	Decision Short	Decision Long	Confirmation Short	Confirmation Long
1. Decision Short	1	0	0	0
2. Decision Long	0	1	0	0
3. Confirmation Short	0	0	1	0
4. Confirmation Long	0	0	0	1
5. Decision Short - Decision Long	1	-1	0	0
6. Decision Long - Decision Short	-1	1	0	0
7. Confirmation Short - Confirmation Long	0	0	1	-1
8. Confirmation Long - Confirmation Short	0	0	-1	1

Table 3. GLM1 design

In the second model (GLM2), we will test the first part of the main hypothesis 3 (positive parametric modulation of the valuation network with reward magnitude of delayed option). As such, we model two event regressors: one from the decision onset and another from the confirmation onset until the onset of the next fixation period. Therefore, the design matrix (Table 4) will contain eight regressors of interest. The group level analysis (contrasts 1-4) will result in the localization of brain regions significantly correlated with the reward magnitude of the delayed option during choice and outcome magnitude during waiting. Again, on a group level we will do a one-sample t-test against the null hypothesis of no activation to test for a group effect while controlling for random effects (subjects) to address the main hypothesis 3. Timecourses of activation from representative magnitude-sensitive regions will then be binned by high, medium, and low magnitudes to see whether such regions respond or not to different levels of magnitude during choice and waiting (as in Figure 3: Ballard and Knutson, 2009). The contrasts 5-8 will show which of the magnitude-sensitive regions are activated stronger in Short (Long).

Regressors ->	Decision Short	Decision Short Mag	Decision Long	Decision Long Mag	Confirmation Short	Confirmation Short Outcome Mag	Confirmation Long	Confirmation Long Outcome Mag
1. Decision Short Mag	0	1	0	0	0	0	0	0
2. Decision Long Mag	0	0	0	1	0	0	0	0
3. Confirmation Short Mag	0	0	0	0	0	1	0	0
4. Confirmation Long Mag	0	0	0	0	0	0	0	1
5. Decision Short Mag - Decision Long Mag	0	1	0	-1	0	0	0	0
6. Decision Long Mag - Decision Short Mag	0	-1	0	1	0	0	0	0
7. Confirmation Short Outcome Mag - Confirmation Long Outcome Mag	0	0	0	0	0	1	0	-1
8. Confirmation Long Outcome Mag - Confirmation Short Outcome Mag	0	0	0	0	0	-1	0	1

Table 4. GLM2 design

In the third model (GLM3), the design matrix will be similar to GLM2 (where all 'Mag' in GLM2 will be replaced with 'Delay') and the model will test the second part of the main hypothesis 3 (negative parametric modulation of the valuation network with delay duration during the choice epoch) and weaker hypothesis 1 (concerning parametric modulation by delay of the executive control network during choice epoch). Additionally, this model should reveal the neural substrate of waiting and address weaker

hypothesis 2 (parametric modulation by delay of anterior prefrontal cortex during the waiting period). The group level analysis will result in the localization of brain regions significantly correlated with the delay magnitude of the delayed option. Timecourses of activation from representative delay-sensitive regions will then be binned by high, medium, and low delay durations to see whether such regions respond or not to different levels of delay during choice and waiting (as in Figure 3: Ballard and Knutson, 2009). The contrasts 5-8 will show which of the delay-sensitive regions are activated stronger in Short (Long). We understand that the regressor for 'confirmation +' epoch will not be sensitive to different time signatures of activity (i.e. it might pick up the peak of activity of waiting-sensitive regions, but lose the ramp speed).

In the forth model (GLM4), we investigate in which regions BOLD signal predicts the *SV* on each trial and whether these regions differed in long and short conditions, i.e. test the main hypothesis 3. Using individual discount factors $\log(k)$ we compute *SV* for each trial. We model an event regressor (from the decision onset till the button press) and a parametric modulation of this regressor by *SV* separately for long and short conditions. Then, the design matrix (Table 5) will contain four regressors of interest. On the group level we will run Decision Short *SV* $>$ Decision Long *SV* (and the opposite) contrast with difference in discount rate between conditions as a between-subject covariate (de-meaned), to see if individual differences in *SV* coding between conditions at the time of choice could explain the extent of the behavioral effect and, thus, address hypothesis 2 (as in Lempert et al., 2017). In FSL FEAT this will be done by adding to a third level analysis with contrast of interest (e.g. Decision Short *SV* $>$ Decision Long *SV*) for each subject as a regressor 1 an extra de-meaned regressor (regressor 2, $|\log(k_S) - \log(k_L)|$) and running a [0 1] contrast. Then the significant contrast will mean the positive linear relationship (slope) between the behavioral measure (absolute difference in $\log(k)$) and BOLD activation (difference in *SV*-sensitive regions between short and long tasks).

Regressors ->	Decision Short	Decision Short *SV*	Decision Long	Decision Long *SV*
1. Decision Short *SV*	0	1	0	0
2. Decision Long *SV*	0	0	0	1
3. Decision Short *SV* - Decision Long *SV*	0	1	0	-1
4. Decision Long *SV* - Decision Short *SV*	0	-1	0	1

Table 5. GLM4 design

8.1.1 Region of Interest (ROI) Analysis

ROI analysis will focus on the valuation network. We will use the conjuction mask from Hare et al. (2014) (http://www.rnl.caltech. edu/resources/index.html). This mask includes voxels in ventromedial prefrontal cortex, ventral striatum, and posterior cingulate cortex. In particular, we will address hypothesis 1 by extracting *t*-statistic map for this ROI for contrasts 1 and 2 from the GLM1 for each participant. Then, for each participant, we will run a correlation across all voxels in this region to see how similar the pattern of activation was during the short and the long tasks.

From GLM2, GLM3 and GLM4 for the peak voxels in the ROI we get the value of the parameter estimates for reward, delay, waiting and *SV* 1) averaged across participants for the short and the long tasks (separately for decision and confirmation events) and run a one-sample t-test to address hypothesis 1; and 2) averaged across groups of participants by discount factor similarity across short and long tasks (two groups: closest to the fitted line of $\log(k_S)$ vs. $\log(k_L)$ and furthest) separately for decision and confirmation events and run a two-sample t-test to compare the groups (hypothesis 2).

8.1.2 Individual Differences Analysis

While localization analyses mainly test for group effects and control for individual differences, individual difference analysis will address variations between subjects. Specifically using GLM (2-4) parameter estimates we will examine whether individuals' neural responsiveness to reward magnitude, delay, waiting and *SV* correlates with their discount factor $\log(k)$. For individual difference analyses, we will extract the parameter estimates (in the form of β coefficients) for the parametric modulated whole-brain regressors from individuals' regional volumes of interest identified in the group localization analyses. These coefficients will index an individuals' neural sensitivity to variables of interest. Averaged coefficients for

each volume of interest will then be correlated against the individuals' tendency to discount the future option, $\log(k)$ (as in Figure 4: Ballard and Knutson, 2009). This individual-level analysis will test the main hypothesis 4. Averaged β coefficients for short and long tasks will also be used to calculate the absolute difference between 'brain' short vs. long and 'behavior' short vs. long (absolute difference between $\log(k)$ in short and long tasks) to plot the correlation between the two and address the main hypothesis 2.

8.2 Multi-voxel pattern Analysis, MVPA

With MVPA, we will examine to what extent the short and long tasks evoke similar neural patterns. Finding a higher correlation between 'brain' short vs. long and 'behavior' short vs. long is the key in our GLM analysis. However, if we do not see it, then there is no strong evidence for no overlap, thus, a better technique, such as MVPA, can address our needs.

8.2.1 Representational Similarity Analysis, RSA

We will use RSA (RSA toolbox for Matlab Nili et al., 2014) to examine the encoding of waiting, postponing, short and long tasks in multi-voxel patterns. This technique uses the Pearson correlational distance, which is insensitive to changes of overall activation magnitude, therefore, makes the RSA orthogonal to the univariate GLM analysis (Walther et al., 2016).

For RSA we will follow Zhang et al. (2017) and adapt their codes available online (github repository). As a part of our planned analysis we will use this methodology combined with a whole-brain "searchlight" procedure (Kriegeskorte et al., 2006), in which we will examine patterns in the immediate neighborhood of every voxel (a 27-voxel cube with that voxel as the center) in the brain. This procedure will allow us to find where in the brain certain task-related variables are encoded, except that now we will focus on the multi-voxel pattern of activation, rather than the activation magnitude in single voxels after GLM. We will use GLM1 first level to extract beta values for four conditions (short decision, long decision, short confirmation until the end of the trial including waiting, long confirmation). Therefore, the activation patterns of an m-voxel searchlight for all 4 conditions of interest can be represented by 4 m-dimensional vectors of beta coefficients. For each searchlight, we will generate a 4 x 4 neural representational dissimilarity matrix (neural RDM) for each individual participant, based on the Pearson correlation distance between activity patterns for all possible pairs of conditions. Specifically, to address hypothesis 2, we can plot difference between discount rates in short and long against similarity between short and long decision (Fisher's z). The short vs. long decision phase model will test for overlap and, therefore, might better address hypothesis 1. We will also compare the neural RDMs to hypothesized dissimilarities in neural patterns between conditions based on a model that accounts for similarity between choice epoch of the short and long tasks but differentiates between waiting and postponing epochs.

8.2.2 Support Vector Regression, SVR

Even if we find a significant overlap in neural networks related to long and short tasks this might not be a strong evidence for a common code. In order to check whether these representations are distinct at a more fine-grained level we plan to use cross-categorical decoding approach (as in Kobayashi and Hsu, 2019). We will follow the analysis steps used in the paper above for individual decoding analysis (except for estimating "group-level utility function"). We will use results from the GLM1 first level as inputs in the decoding analysis. In our planned analysis we will ask i) if we could decode trial-by-trial individual *SV* from voxel-wise BOLD signals in a searchlight (10-mm radius) using one-run-leave-out five-hold cross-validation and support vector regression (SVR) within Long and Short tasks (two categories) separately; ii) if we could predict individual *SV* in Long task via SVR trained based on *SV* in Short task and vice versa.

8.3 Further exploratory analyses

Following the GLM, ROI and MVPA planned analyses we would like to take advantage of the techniques that appeared recently:

- joint modeling' approach (Palestro et al., 2018) that takes into account covariation between the neural and behavioral models. The main assumption is that some areas of the brain (e.g. in valuation or executive control network) are positively related to the probability of the choice of delayed (or immediate) option.

- since we are using hierarchical Bayesian modeling to estimate discount factors, it's reasonable to consider hierarchical Bayesian analysis of BOLD (instead of a standard GLM described earlier; (Molloy et al., 2018)).

9 ACKNOWLEDGEMENTS

The pre-registration is done according to the template provided by Jessica Flannery available on OSF (https://osf.io/6juft/), and according to recommendations from Poldrack et al. (2008) and Nichols et al. (2017).

We acknowledge an outstanding undergraduate student who helped us to start this project: Danielle John from CUNY Hunter College.

This research program is supported by The Program for Eastern Young Scholar at Shanghai Institutions of Higher Learning to EL and NSFC Young Scholar Grant (31750110461) to EL.

REFERENCES

Ballard, K. and Knutson, B. (2009). Dissociable neural representations of future reward magnitude and delay during temporal discounting. *NeuroImage*, 45(1):143–150.

Chen, Z., Guo, Y., Zhang, S., and Feng, T. (2019). Pattern classification differentiates decision of intertemporal choices using multi-voxel pattern analysis. *Cortex*, 111:183–195.

Cox, R. W. (1996). AFNI: Software for Analysis and Visualization of Functional Magnetic Resonance Neuroimages. *Computers and Biomedical Research*, 29(3):162–173.

Deichmann, R., Gottfried, J., Hutton, C., and Turner, R. (2003). Optimized EPI for fMRI studies of the orbitofrontal cortex. *NeuroImage*, 19(2):430–441.

Esteban, O., Birman, D., Schaer, M., Koyejo, O. O., Poldrack, R. A., and Gorgolewski, K. J. (2017). MRIQC: Advancing the automatic prediction of image quality in MRI from unseen sites. *PLOS ONE*, 12(9):e0184661.

Esteban, O., Markiewicz, C. J., Blair, R. W., Moodie, C. A., Isik, A. I., Erramuzpe, A., Kent, J. D., Goncalves, M., DuPre, E., Snyder, M., Oya, H., Ghosh, S. S., Wright, J., Durnez, J., Poldrack, R. A., and Gorgolewski, K. J. (2019). fMRIPrep: a robust preprocessing pipeline for functional MRI. *Nature Methods*, 16(1):111–116.

Furnham, A. and Boo, H. C. (2011). A literature review of the anchoring effect. *The Journal of Socio-Economics*, 40(1):35–42.

Golsteyn, B. H., Grönqvist, H., and Lindahl, L. (2014). Adolescent time preferences predict lifetime outcomes. *The Economic Journal*, 124(580):F739–F761.

Gregorios-Pippas, L., Tobler, P. N., and Schultz, W. (2009). Short-Term Temporal Discounting of Reward Value in Human Ventral Striatum. *Journal of Neurophysiology*, 101(3):1507–1523.

Hare, T. A., Hakimi, S., and Rangel, A. (2014). Activity in dlPFC and its effective connectivity to vmPFC are associated with temporal discounting. *Frontiers in Neuroscience*, 8.

Jenkinson, M., Beckmann, C. F., Behrens, T. E., Woolrich, M. W., and Smith, S. M. (2012). FSL. *NeuroImage*, 62(2):782–790.

Jimura, K., Chushak, M. S., and Braver, T. S. (2013). Impulsivity and self-control during intertemporal decision making linked to the neural dynamics of reward value representation. *Journal of Neuroscience*, 33(1):344–357.

Kable, J. W. and Glimcher, P. W. (2007). The neural correlates of subjective value during intertemporal choice. *Nature Neuroscience*, 10(12):1625–1633.

Kable, J. W. and Glimcher, P. W. (2010). An "As Soon As Possible" Effect in Human Intertemporal Decision Making: Behavioral Evidence and Neural Mechanisms. *Journal of Neurophysiology*, 103(5):2513–2531.

Kobayashi, K. and Hsu, M. (2019). Common neural code for reward and information value. *Proceedings of the National Academy of Sciences*, 116(26):13061–13066.

Kriegeskorte, N., Goebel, R., and Bandettini, P. (2006). Information-based functional brain mapping. *Proceedings of the National Academy of Sciences*, 103(10):3863–3868.

Lempert, K. M., Speer, M. E., Delgado, M. R., and Phelps, E. A. (2017). Positive autobiographical memory retrieval reduces temporal discounting. *Social Cognitive and Affective Neuroscience*, 12(10):1584–1593.

Lempert, K. M., Steinglass, J. E., Pinto, A., Kable, J. W., and Simpson, H. B. (2018). Can delay discounting deliver on the promise of RDoC? *Psychological Medicine*, pages 1–10.

Lukinova, E., Wang, Y., Lehrer, S. F., and Erlich, J. C. (2019). Time preferences are reliable across time-horizons and verbal versus experiential tasks. *eLife*, page 27.

Massar, S. A., Libedinsky, C., Weiyan, C., Huettel, S. A., and Chee, M. W. (2015). Separate and overlapping brain areas encode subjective value during delay and effort discounting. *NeuroImage*, 120:104–113.

McClure, S. M., Ericson, K. M., Laibson, D. I., Loewenstein, G., and Cohen, J. D. (2007). Time Discounting for Primary Rewards. *Journal of Neuroscience*, 27(21):5796–5804.

McClure, S. M., Laibson, D. I., Lowenstein, G., and Cohen, J. D. (2004). Separate Neural Systems Value Immediate and Delayed Monetary Rewards. *Science*, 306(5695):503–507.

Mischel, W., Shoda, Y., and Rodriguez, M. (1989). Delay of gratification in children. *Science*, 244(4907):933–938.

Molloy, M. F., Bahg, G., Li, X., Steyvers, M., Lu, Z.-L., and Turner, B. M. (2018). Hierarchical Bayesian Analyses for Modeling BOLD Time Series Data. *Computational Brain & Behavior*, 1(2):184–213.

Nichols, T. E., Das, S., Eickhoff, S. B., Evans, A. C., Glatard, T., Hanke, M., Kriegeskorte, N., Milham, M. P., Poldrack, R. A., Poline, J.-B., Proal, E., Thirion, B., Van Essen, D. C., White, T., and Yeo, B. T. T. (2017). Best practices in data analysis and sharing in neuroimaging using MRI. *Nature Neuroscience*, 20(3):299–303.

Nili, H., Wingfield, C., Walther, A., Su, L., Marslen-Wilson, W., and Kriegeskorte, N. (2014). A Toolbox for Representational Similarity Analysis. *PLoS Computational Biology*, 10(4):e1003553.

Onoda, K., Okamoto, Y., Kunisato, Y., Aoyama, S., Shishida, K., Okada, G., Tanaka, S. C., Schweighofer, N., Yamaguchi, S., Doya, K., and Yamawaki, S. (2011). Inter-individual discount factor differences in reward prediction are topographically associated with caudate activation. *Experimental Brain Research*, 212(4):593–601.

Paglieri, F. (2013). The costs of delay: Waiting versus postponing in intertemporal choice. *Journal of the Experimental Analysis of Behavior*, 99(3):362–377.

Palestro, J. J., Bahg, G., Sederberg, P. B., Lu, Z.-L., Steyvers, M., and Turner, B. M. (2018). A tutorial on joint models of neural and behavioral measures of cognition. *Journal of Mathematical Psychology*, 84:20–48.

Palombo, D. J., Keane, M. M., and Verfaellie, M. (2015). The medial temporal lobes are critical for reward-based decision making under conditions that promote episodic future thinking: DECISION MAKING IN AMNESIA. *Hippocampus*, 25(3):345–353.

Peirce, J. W. (2007). PsychoPy—psychophysics software in Python. *Journal of neuroscience methods*, 162(1):8–13.

Peters, J. and Büchel, C. (2010). Episodic Future Thinking Reduces Reward Delay Discounting through an Enhancement of Prefrontal-Mediotemporal Interactions. *Neuron*, 66(1):138–148.

Poldrack, R. A., Fletcher, P. C., Henson, R. N., Worsley, K. J., Brett, M., and Nichols, T. E. (2008). Guidelines for reporting an fMRI study. *NeuroImage*, 40(2):409–414.

Prevost, C., Pessiglione, M., Metereau, E., Clery-Melin, M.-L., and Dreher, J.-C. (2010). Separate Valuation Subsystems for Delay and Effort Decision Costs. *Journal of Neuroscience*, 30(42):14080–14090.

Tanaka, S. C., Yamada, K., Yoneda, H., and Ohtake, F. (2014). Neural Mechanisms of Gain-Loss Asymmetry in Temporal Discounting. *Journal of Neuroscience*, 34(16):5595–5602.

Tversky, A. and Kahneman, D. (1974). Judgment under Uncertainty: Heuristics and Biases. *Science*, 185(4157):1124–1131.

van den Bos, W., Rodriguez, C. A., Schweitzer, J. B., and McClure, S. M. (2014). Connectivity Strength of Dissociable Striatal Tracts Predict Individual Differences in Temporal Discounting. *Journal of Neuroscience*, 34(31):10298–10310.

Walther, A., Nili, H., Ejaz, N., Alink, A., Kriegeskorte, N., and Diedrichsen, J. (2016). Reliability of dissimilarity measures for multi-voxel pattern analysis. *NeuroImage*, 137:188–200.

Watts, T. W., Duncan, G. J., and Quan, H. (2018). Revisiting the Marshmallow Test: A Conceptual Replication Investigating Links Between Early Delay of Gratification and Later Outcomes. *Psychological Science*, page 0956797618761661.

Wilson, T. D., Houston, C. E., Etling, K. M., and Brekke, N. (1996). A New Look at Anchoring Effects:

Basic Anchoring and Its Antecedents. *Journal of Experimental Psychology: General*, 125(4):16.

Wittmann, M., Lovero, K. L., Lane, S. D., and Paulus, M. P. (2010). Now or later? Striatum and insula activation to immediate versus delayed rewards. *Journal of Neuroscience, Psychology, and Economics*, 3(1):15–26.

Woolrich, M. W., Ripley, B. D., Brady, M., and Smith, S. M. (2001). Temporal Autocorrelation in Univariate Linear Modeling of FMRI Data. *NeuroImage*, 14(6):1370–1386.

Zhang, Z., Fanning, J., Ehrlich, D. B., Chen, W., Lee, D., and Levy, I. (2017). Distributed neural representation of saliency controlled value and category during anticipation of rewards and punishments. *Nature Communications*, 8(1).